Supplemental Document

optica

Time-magnified photon counting with 550-fs resolution: supplement

BOWEN LI,[1,2] JAN BARTOS,[1] YIJUN XIE,[1] AND SHU-WEI HUANG[1,*]

[1] *Department of Electrical, Computer, and Energy Engineering, University of Colorado, Boulder, Colorado 80309, USA*
[2] *e-mail: Bowen.Li@colorado.edu*
[*] *Corresponding author: Shu-Wei.Huang@colorado.edu*

Supplement DOI: https://doi.org/10.6084/m9.figshare.15028917

Parent Article DOI: https://doi.org/10.1364/OPTICA.420816

Supplementary Material

optica

Time-magnified photon counting with a 550-fs resolution: supplementary material

Bowen Li,[1] Jan Bartos, Yijun Xie, and Shu-Wei Huang*

Department of Electrical, Computer, and Energy Engineering, University of Colorado, Boulder, Colorado, US
[1] *Email: Bowen.Li@colorado.edu*
**Corresponding author: Shu-Wei Huang@colorado.edu*

Published 17 August 2021

This document provides supplementary information to "Time-magnified photon counting with a 550-fs resolution," https://doi.org/10.1364/OPTICA.420816. It consists of four sections: 1. TM-TCSPC schematic diagram; 2. Resolving sub-ps pulsewidth change with TM-TCSPC; 3. ToF image and signal processing; and 4. Photon pile-up effect.

1. TM-TCSPC schematic diagram

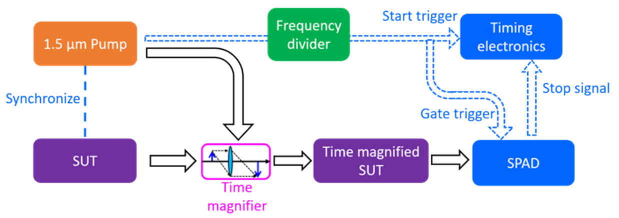

Fig. S1. The schematic diagram for the TM-TCSPC. SUT, signal under test; SPAD, single-photon avalanche diodes.

Since the set-up schematic in Fig. 2 focuses on the fiber parametric temporal magnifier, more details on TM-TCSPC measurement configuration are provided in Fig. S1. Since a 100 MHz pump source was used for both pumping the temporal magnifier and generating the 1.2-µm signal under test (SUT), the output signal from the temporal magnifier also had a repetition rate of 100 MHz. However, the SPAD used in the experiment (MPD, PDM-IR) only supported a maximum trigger frequency of 25 MHz when operating at gated mode. To synchronize the gate window of the SPAD with the optical input signal, 1 % of the 1.5-µm source was received by a photodetector to generate a 100 MHz electrical pulse train, which was then frequency divided by 4 times using an electrical frequency divider to generate a 25-MHz electrical pulse train as the trigger. This trigger was then split equally into two parts. One part served as the gate trigger to synchronize the gate window in the SPAD, while the other part was used as the start trigger for the timing electronics module (Hydraharp 400). Once the SPAD detects a photon, a stop signal would be generated and sent to the timing electronics module, registering the photon in the time bin. The instrument response function (IRF) of the whole TCSPC system was measured to be 90 ps using fs pulses.

2. Resolving sub-ps pulsewidth change with TM-TCSPC

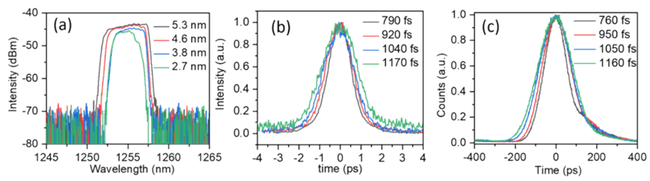

Fig. S2. Resolving sub-ps pulsewidth change with TM-TCSPC. (a) Optical spectra of the input pulses with different bandwidths. (b) Background-free SHG intensity autocorrelation traces of the corresponding pulses. Legends show the measured pulsewidth after deconvolution (c) TM-TCSPC timing histograms of the corresponding pulses. Legends show the measured pulsewidth after demagnification and deconvolution.

As shown in Fig. S2(a), the different pulsewidths used in Fig. 4 were obtained by varying the optical bandwidth using a variable bandpass filter. Four different bandwidths: 2.7 nm, 3.8 nm, 4.6 nm, and 5.3 nm were used for the test. Before the direct measurements using TM-TCSPC, pulsewidths were first characterized using a background-free second harmonic generation (SHG) intensity autocorrelator (AC) as references and the autocorrelation traces are shown in Fig. S2(b). The AC measured full-width at half maximum (FWHM) W_{AC} after deconvolution and Gaussian fitting were 790 fs, 920 fs, 1040 fs, and 1170 fs respectively, and are regarded as the ground truth of pulsewidth. The change of pulsewidth in each step was only around 130 fs. Then, the pulses were measured again using the TM-TCSPC with the timing histograms shown in Fig. S2 (c). To obtain the pulsewidth, the TM-TCSPC results needed to be demagnified by the temporal magnification ratio and then deconvolved with the system IRF. The demagnified FWHM of TM-TCSPC histograms ($W_{\text{TM-TCSPC}}$) in Fig. S2(c) were obtained to be 940 fs, 1100 fs, 1190 fs and 1280 fs respectively. The IRF of TM-TCSPC can then be calculated through deconvolution under Gaussian approximation as IRF=$(W^2_{\text{TM-TCSPC}}\text{-}W^2_{\text{AC}})^{1/2}$ using any set of the four pulsewidth. However, the dispersion slope of dispersive fibers in the system induced finite bandwidth-dependent distortions on the TM-TCSPC histogram, as can be observed on Fig. S2(c) where the most obvious distortion is shown on the black trace. Such distortions led to some IRF calculation deviation ranging from 500 fs to 600 fs. To take such influence into consideration, a fitted IRF that minimized the r.m.s. difference between the two methods was calculated to be 550 fs by numerically solving

$$\min_{\mathrm{IRF}} \sqrt{\frac{1}{4}\sum_{4}^{1} i\left(\sqrt{Wi^2_{TM-TCSPC}-\mathrm{IRF}^2}-Wi_{AC}\right)^2},$$

where $Wi_{\text{TM-TCSPC}}$ and Wi_{AC} refer to the four TM-TCSPC histogram width and four AC measured puslewidth, respectively. Based on the fitted IRF, the measured pulsewidth using TM-TCSPC were 760 fs, 950 fs, 1050 fs, and 1160 fs, respectively, and the corresponding r.m.s. deviation from the ground truth was only 22 fs.

3. ToF image and signal processing

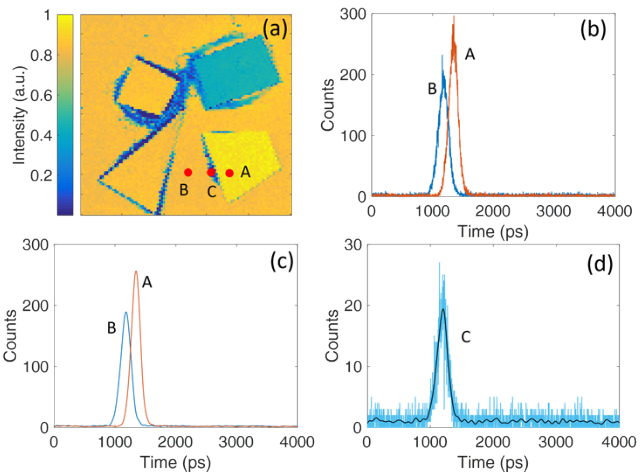

Fig. S3. (a) Intensity image of the glass sample. (b) Original timing histogram obtained by TM-TCSPC system at two different positions marked on (a). (c) Processed timing histogram using low-pass filtering in the frequency domain. (d) Original and processed timing histograms at point C in (a).

The sample was mounted on a motorized 2D translation stage and was scanned across a 10 mm by 10 mm area through 10,000 steps for imaging. 1.2-µm signal with 5-nm bandwidth was focused onto the sample. The intensity image shown in Fig. S3(a) was obtained from the peak height of the photon-histogram using conventional TSCPC. The different intensities observed at each glass sample were due to the limited working distance of the focusing lens. Lower reflected power was collected for surfaces that are slightly out of focus. Besides, near-zero intensities were measured at few pixels on the glass edges, owing to the tilted surface. Other low-intensity areas outside the glass edges were caused by the coating defects. However, the ToF depth imaging should not be influenced by the intensity variation since only height contrasts are measured. The raw data obtained using TM-TCSPC at two different points A and B marked by red dots in Fig. S3(a) is shown by the orange and blue trace in Fig. S3(b), respectively. Both timing histograms were acquired with an integration time of 0.3 s and the bin size for the histograms was 2 ps. As can be observed, the two timing histograms are well separated. To further increase the accuracy in determining the peak location, both traces were filtered in the frequency domain with a bandwidth of 10 GHz. The filtered traces are shown in Fig. S3(c), which show a much higher signal-to-noise ratio (SNR). According to Fig. S3(c), temporal separation of 166 ps was found between the two histograms, which correspond to a height difference of 190 µm. The histogram for point C where the defective coating induces a 10 dB less reflectivity is shown in Fig. S3(d). Even though the original histogram exhibits much worse SNR owing to a lower number of photon counts, the black trace after filtering still shows sufficient SNR to precisely locate the peak location.

4. Photon pile-up effect

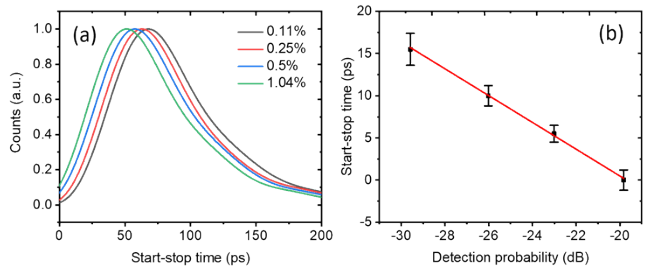

Fig. S4. Investigation of pile-up effect on the error of the TCSPC timing histogram. (a) Four timing histograms with different detection probability. (b) Peak locations of the timing histograms with respect to the detection probability. Linear fitting shows a peak shift of -1.6 ps/dB. Four repeated measurements were performed for each detection probability to obtain the mean value and standard deviation.

The large depth measurement error observed in Fig. 5(c) is attributed to the photon pile-up effect. To further confirm our hypothesis, an experiment was conducted by launching quantum level femtosecond pulses at 1.5 µm directly into the SPAD. A continuously variable metallic neutral density filter (Thorlabs, NDC-25C-2) was used to change the detection probability while all other experimental conditions were kept the same. A longer integration time of 10 s was used to further increase the SNR to guarantee the measurement accuracy. Four different detection probabilities were used for the test: 0.11%, 0.25%, 0.50% and 1.04%. The corresponding TCSPC timing histograms are shown in Fig. S4(a). Obvious timing shifts are observed at different detection probabilities. For each detection probability, four repeated measurements were performed to obtain the mean and standard deviation of the peak locations of the TCSPC timing histograms. The results are shown in Fig. S4(b). A monotonic timing shift towards shorter time can be observed with increasing detection probability. Around 15-ps timing shift was introduced when the detection probability was increased from 0.11 % to 1.04 %. The slope from the linear fitting is -1.6 ps/dB. Therefore, we confirm that photon pile-up effect can induce picosecond scale shift on the TCSPC timing histograms even when the detection probability is below 1%, which is detrimental for mm and sub-mm scale ToF depth imaging. From this perspective, the mitigation effect from the TM-TCSPC technique is important for achieving accurate measurement results.